JOURNAL OF SPACECRAFT AND ROCKETS
Vol. 48, No. 2, March–April 2011

Damage of Ti-6Al-4V Alloy Induced by Hypervelocity Impact

S. L. Dong,* Z. Y. Ye,† H. B. Geng,‡ H. Zhang,§ Y. Zou,§ D. Z. Yang,¶ and S. Y. He¶
Harbin Institute of Technology, 150001 Harbin, People's Republic of China
and
E. H. Han**
Chinese Academy of Sciences, 110016 Shenyang, People's Republic of China

DOI: 10.2514/1.49458

The impact of macro- and microdamage behaviors of Ti-6Al-4V alloy has been examined using a two-stage light gas gun. Disks with thicknesses from 2 to 20 mm cut from a forged and annealed Ti-6Al-4V alloy bar with the diameter of 70 mm, and plates cut from a rolled Ti-6Al-4V alloy sheet with a thickness of 1 mm, were employed as single- and multilayer targets, respectively. The impact velocities of the spherical steel, 4.0-mm-diam projectiles, ranged from 1 to 4 km/s. For the impacted targets, the crater shape and dimension, microstructures and microhardness distributions in the vicinity of craters were characterized by complementary techniques such as optical microscopy, scanning electron microscopy, and Vickers microhardness measuring. Based on the experimental results, the penetration resistance of the annealed Ti-6Al-4V alloy and the critical impact velocity to form the debris clouds in the Ti-6Al-4V alloy sheet were obtained.

Nomenclature

v = impact velocity

I. Introduction

AS A promising metallic structural material, Ti-6Al-4V alloy has been widely applied in space industry due to its high specific strength and stiffness, excellent corrosion resistance and environmental stability [1,2]. With the expansion of space exploration, the hazards from hypervelocity impacts by meteoroids or orbital debris would be more concerned for spacecraft development, design and operation [3]. Therefore, it is essential to understand the hypervelocity impact effects on Ti-6Al-4V alloy for its better application in spacecraft parts. Many attempts [4–13] in fact have been made to examine the impact response of Ti-6Al-4V alloy at from low velocity to hypervelocity achieved by various accelerating techniques in laboratory such as powder gun [5,6], barrel gun [7–10,12], conical shaped charge liners [13], light gas gun [11] and two-stage gas gun [4]. The aim of these studies was either for space application consideration [4,5], scientific investigation [6–11] or for making armors [12,13]. However, up to the present, the obtained knowledge is not sufficient enough to enable spacecraft engineers gaining a better understanding of hypervelocity impact processes or to allow them to make more effective shielding design. In this case, systemic and detailed work is still necessary for learning more phenomena of hypervelocity impact in Ti-6Al-4V alloy.

Based on a standard two-stage gas gun in School of Materials Science and Engineering, Harbin Institute of Technology, China, many investigations have been carried out on the hypervelocity impact effects on typical structural materials such as aluminum, magnesium and titanium alloys, high strength steel, and carbon fiber reinforced epoxy matrix composite in recent years. Following the previous efforts, this work aims at studying the macro- and microdamages of Ti-6Al-4V alloy produced by hypervelocity impact using this two-stage gas gun, optical and electron metallographic techniques. The experimental results and their outputs obtained in the Ti-6Al-4V alloy targets for various thicknesses and configuration at the impact velocities ranging from about 1 to 4 km/s will be presented hereafter.

Received 24 February 2010; revision received 19 July 2010; accepted for publication 8 September 2010.

*Doctor, School of Materials Science and Engineering; sldong@hit.edu.cn (Corresponding Author).
†Senior Technician, School of Materials Science and Engineering.
‡Doctor, School of Materials Science and Engineering.
§Graduate Student, School of Materials Science and Engineering.
¶Professor, School of Materials Science and Engineering.
**Senior Researcher, Institute of Metal Research.

II. Experimental

A. Experimental Targets

Two milled products of Ti-6Al-4V alloy, the forged round bar with a diameter of 70 mm and rolled sheet with the thickness of 1 mm, were employed as the experimental materials. The quality of the experimental Ti-6Al-4V alloy was strictly controlled in order to meet the requirements for spacecraft parts. The provided forged round bar and rolled sheet were used to machine single-layer (plate) targets and multilayer targets, respectively. The as-forged round bar was cut into disks with various desired thicknesses for single-layer target specimens. After an annealing treatment at 750°C for 60 min, the disks were surface ground and divided into different groups depending on the thickness which was designed as 2, 5, 7, 10, 12 and 20 mm, respectively. The multilayer targets were prepared from the plates with dimension of 100×100 mm cut from the as-rolled Ti-6Al-4V alloy sheet. Four plates were mounted by long screws in the plate corners for making a multilayer target. The distance for each layer plate is 50 mm. The typical target specimens used in the current study are shown in Fig. 1.

B. Impact Testing

In the impact experiments, the 4-mm-diam bearing-steel sphere were used as projectiles to impact the Ti-6Al-4V alloy target specimens at the normal impact model (the projectile direction is normal to the surface of target), in the two-stage light gas gun as shown in Fig. 2. The projectile velocity was measured in the tip of the launch tube using an oscilloscope in a "time of flight" mode. In current study, the impacting velocity is within the range from about 1 to 4 km/s, and the error in measurement of project velocity is about ± 0.15 km/s. One group of single targets were impacted by steel projectiles at a certain velocity of about 2 km/s, and another group of single targets were tested for comparison at nominal velocities of 1, 2, or 3 km/s, respectively. For the multilayer targets, four impacting velocities were selected, namely, 1, 2, 3, and 4 km/s. The actual recorded velocity value during the impact experiment is generally not an integer as proposed, because of the variability in the two-stage light gas gun operation. Figure 3 gives an example of velocity

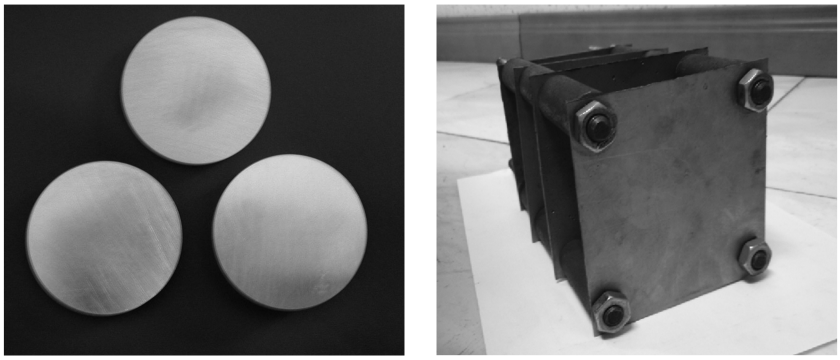

a) Single targets b) Multilayer target

Fig. 1 Target specimens employed for impact test.

Fig. 2 The two-stage light gas gun for impact experiment.

measurement when a Ti-6Al-4V alloy multilayer target specimen was impacted by a 4 mm steel sphere at the designated velocity of 4 km/s. It can be seen that the actually determined value is 4.049 km/s, but for convenience, it is still nominally denoted as 4 km/s in this paper.

C. Damage Analysis

After impact testing, the Ti-6Al-4V alloy targets were carefully checked and photographed. For each single impacted target, the block containing a crater was removed and then cut into two sections along the crater axis to observe the exact cross-section view of crater. One section was used to investigate the profile and dimension (such as crater depth or penetration distance and diameter) of the impacted crater, and the other section was ground, polished and etched for further microexamination. Hence, the morphologies of the crater, microdamage behavior and microstructure development of the Ti-6Al-4V alloy in the vicinity of crater due to hypervelocity impact were characterized using Olympus optical microscope and Hitachi scanning electron microscope. The microhardness distribution in the region close to the crater was evaluated using a HVS-1000 model Vickers hardness tester. A diamond indenter was employed to apply a load of 100 g for 10 s. The damage analysis procedures for the multilayer target specimens were similar to those of the preceding mentioned single targets.

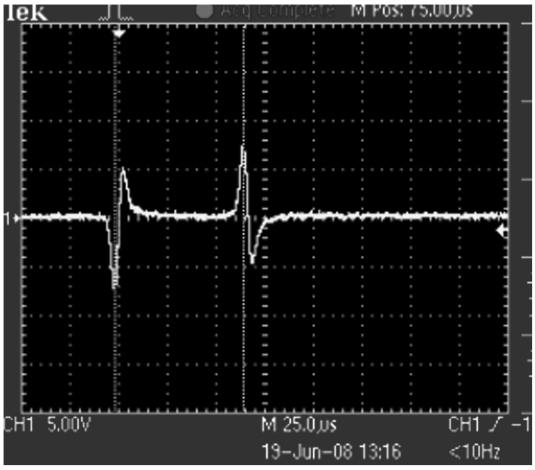

Fig. 3 Determination of projectile velocity by an oscillograph (v= 4.049 km/s).

III. Results and Discussion

A. Macrodamage of Single Targets

Figures 4 and 5 show the front and rear views of the impacted single Ti-6Al-4V alloy targets with various thicknesses at a velocity of about 2 km/s, and the corresponding cross-section views of the impacted targets are given in Fig. 6. It can be seen that the macrodamage patterns and the configuration of the impacted crater on the targets vary with the targets thickness. The 2-mm-thick target was completely penetrated, as shown in Figs. 4a and 5a, namely perforation occurred during impact process. On the contrary, the 5- and 7-mm-thick targets were not completely penetrated (seen in Figs. 4b, 4c, and 6b, respectively), but it can be seen bulging characteristic in the rare surface of the targets, which is obvious for the 5 mm target (Fig. 5b) and appreciably seen for the 7 mm target (Fig. 5c). As the targets thickness is more than 7 mm, only front surface indentation but no rear surface bulge of the samples could be observed, as shown in Figs. 4d and 5d.

Except for the thinner target with 2 mm thickness, the crater profiles formed by spherical 4 mm steel projectile at a nominal velocity of 2 km/s are similar, as depicted in Figs. 4 and 6. Such a crater is composed of a radial symmetry, a raised lip around the edge (indicating the ejecting or outward flow of molten target material) and dark central cavity, implying typical craters formed on ductile surfaces impacted by a spherical projectile. It is well known that the crater configuration formation resulted from interaction of projectile with the target during impact [11,14,15].

In past decades, most of the experimental work on the projectile-target interaction models was done with aluminum as a target [14,15]. A previous investigation by Baker [14], based on analyzing crater morphology and dimension with the relationship of velocity, had identified three different types of craters produced by impact. The first type is an elongated crater with the intact projectile remaining in the crater bottom, which is usually formed at relatively low velocities for very strong and dense projectiles impact weaker targets. The second type is a relative shallower or wider crater, which is commonly formed at appropriate impacting velocities with deformation or destruction of the projectile, for projectiles possessing the equal to or less than the strength and density of the target material, or for strong and dense projectiles impacting weaker targets

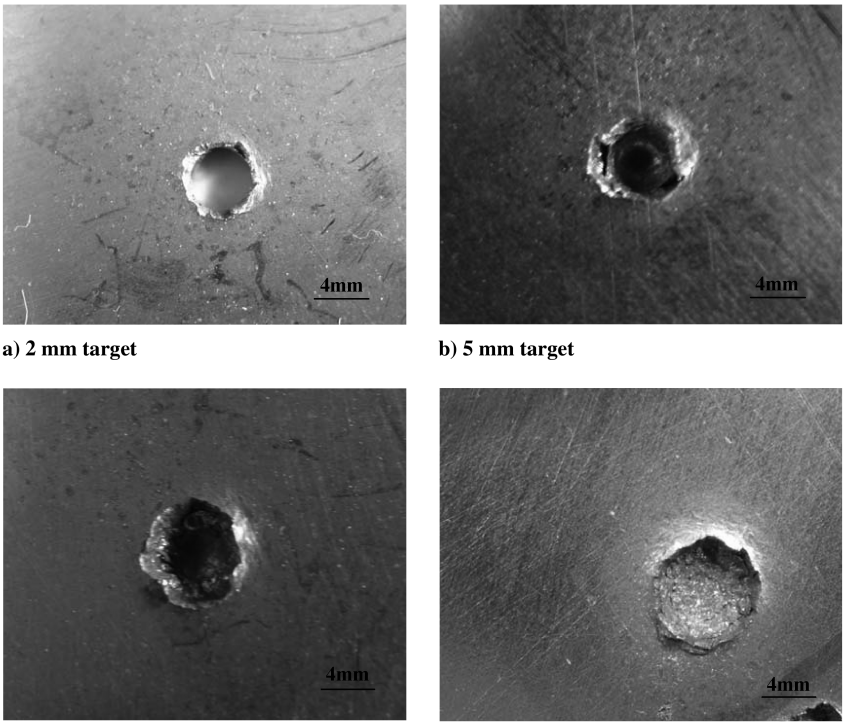

a) 2 mm target b) 5 mm target

c) 7 mm target d) 20 mm target

Fig. 4 Front views of impacted targets with various thicknesses at a nominal velocity of 2 km/s.

at more higher velocities. The third one is the truly hypervelocity crater, usually holding a profile of hemisphere, which is formed above the threshold velocity depending on properties of projectiles and targets. In this case, the complete destruction of the projectile occurs during impacting. A recent work [16] demonstrates that the crater cross-sectional configurations produced by hypervelocity impact are similar for pure aluminum and pure titanium.

According to these studies as well as the profile features described in Figs. 4 and 6, the craters match the second type crater suggested by Baker [14], as induced by impact at 2 km/s in the annealed Ti-6Al-4V alloy targets with the thickness no less than 5 mm.

The depths and diameters of the crater impacted at velocity of 2 km/s in the Ti-6Al-4V alloy targets with different thickness were carefully measured and the obtained data are listed in Table. 1. It can be seen that the crater diameter increases with increasing the target thickness, but the penetration depth or the crater depth firstly increases as the target thickness increases from 2 to 7 mm, and then gradually decreases with the increase of target thickness. In other

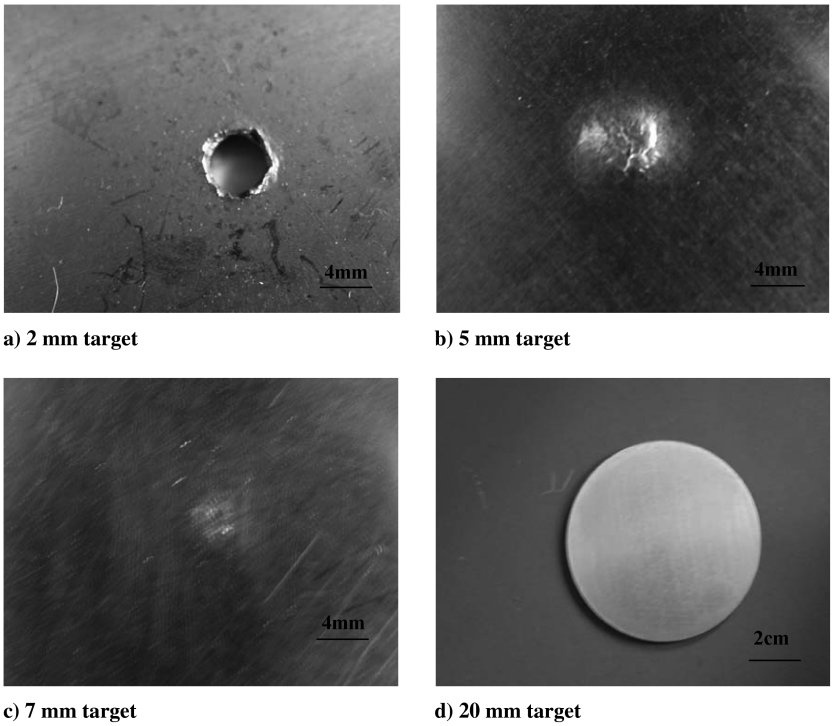

a) 2 mm target b) 5 mm target

c) 7 mm target d) 20 mm target

Fig. 5 Rear views of impacted targets with various thicknesses at a nominal velocity of 2 km/s.

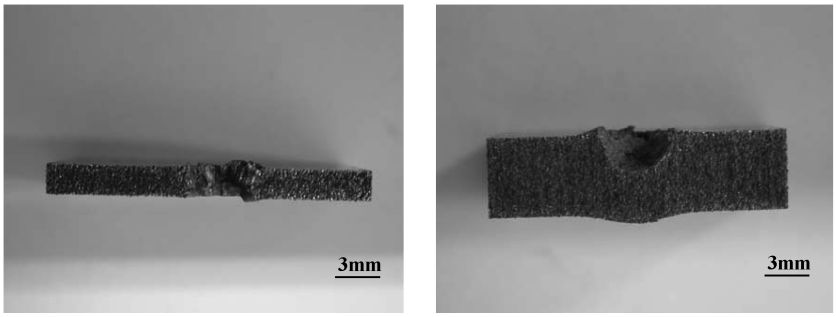

a) 2 mm target b) 5 mm target

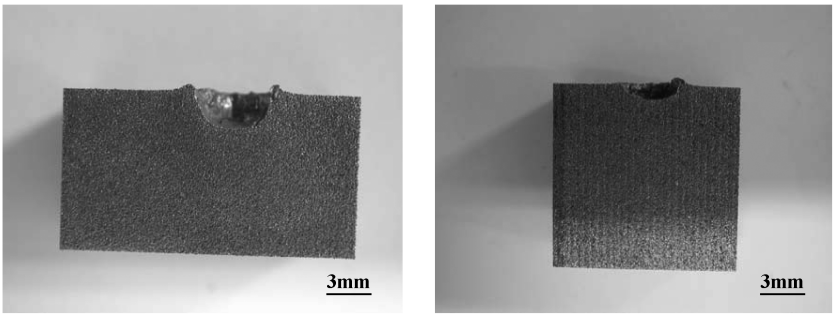

c) 10 mm target d) 20 mm target

Fig. 6 Cross-section views of impacted targets with various thicknesses at a nominal velocity of 2 km/s.

Table 1 Parameters of the craters produced at a nominal velocity of 2 km/s

Target thickness, mm	Crater diameter, mm	Crater depth, mm
2.0	4.90	2.00
5.0	5.37	2.45
7.0	6.28	2.71
10.0	6.32	2.45
12.0	6.68	2.17
20.0	6.98	2.03

words, the crater profile experiences a transition from "hemispherical" to "shallow wide" crater as increasing the target thickness from 7 to 20 mm. Such transition is believed to be resulted from the combined effects of dynamic plastic deformation, dissipation of impact energy, heat generation, high-strain-rate strain hardening and enhanced resistance in the penetrating direction of the Ti-6Al-4V alloy, as well as the possible destruction of steel projectile during the impacting on different thickness targets.

Additional limited tests were preformed in other thickness regime, such as impacting the 20 mm target at the nominal velocities of 1 and

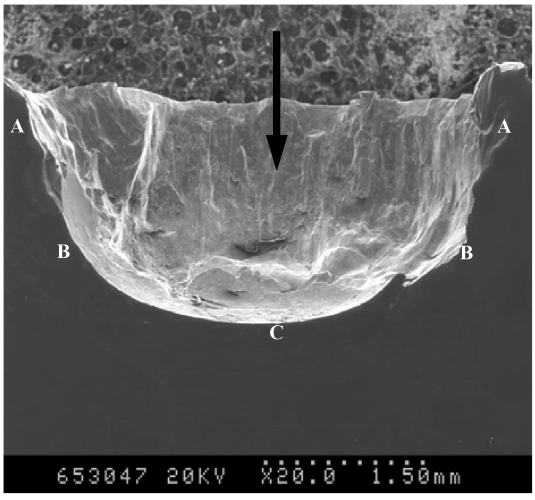

Fig. 7 SEM image showing cross-section view of a crater (12 mm target, 4 mm spherical steel projectile, impacting at 2 km/s).

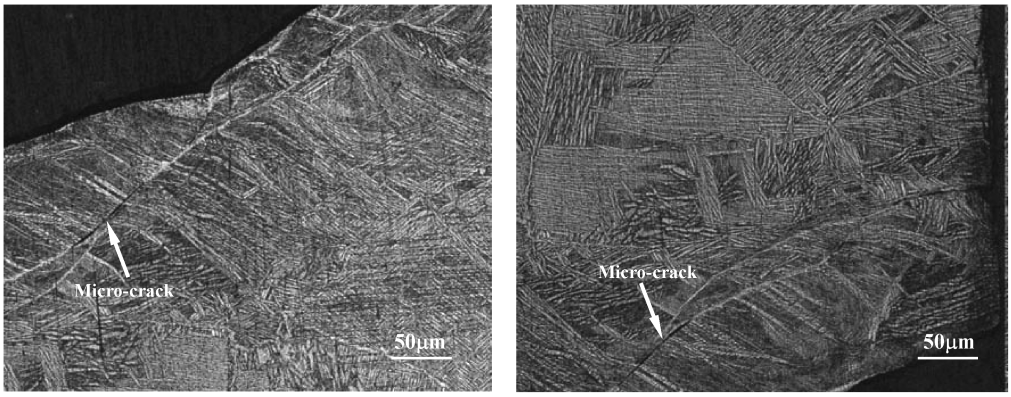

Fig. 8 Optical micrographs showing microcracks and deformation bands in the 2 mm target (4 mm spherical steel projectile, impacting at 2 km/s): a) view near entrance of penetrated hole (left micrograph) and b) view near exit of penetrated hole (right micrograph).

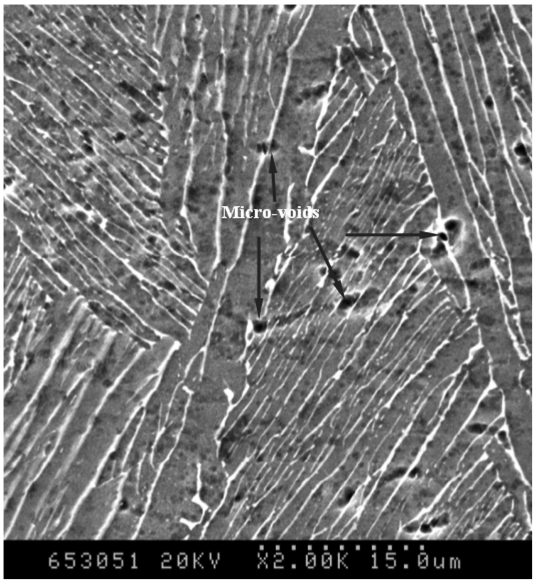

Fig. 9 SEM micrograph showing microvoids in the 5 mm target impacted at 2 km/s.

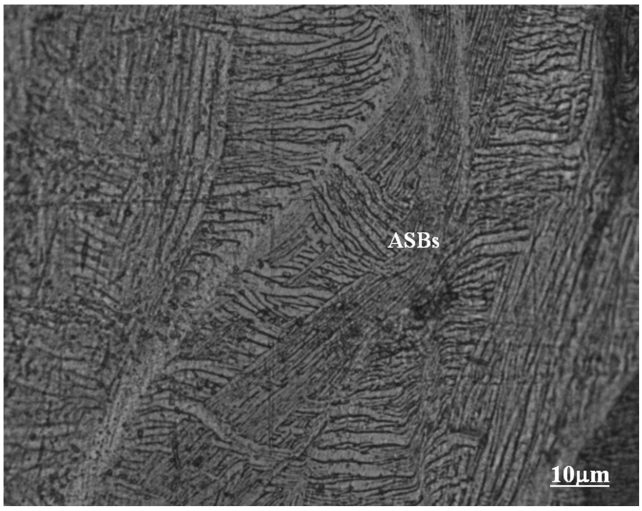

Fig. 10 Optical micrograph showing ASBs formed in the 20 mm target impacted at 2 km/s.

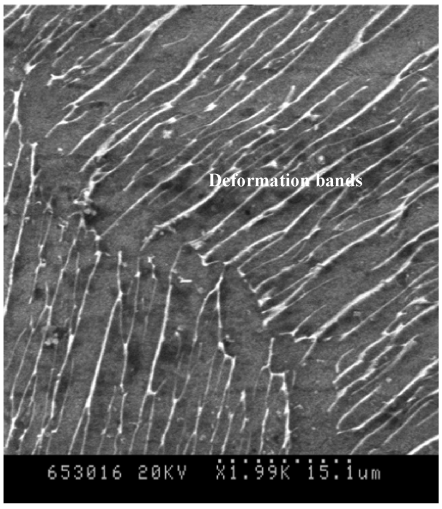

a) View near top of the crater, marked "A" in Fig. 7

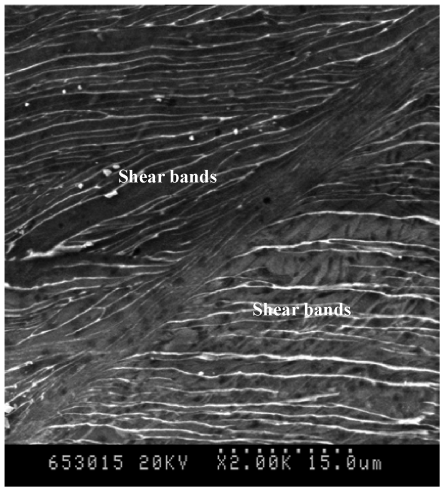

b) View near middle of the crater, marked "B" in Fig. 7

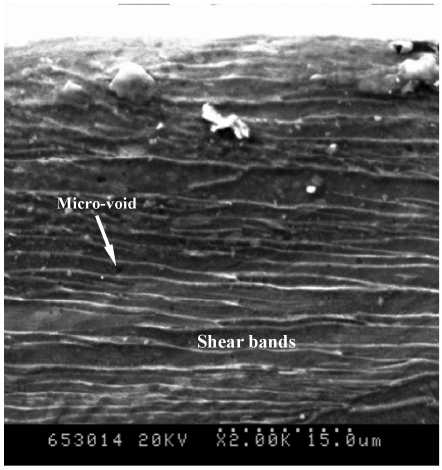

c) View near bottom of the crater, marked "C" in Fig. 7

Fig. 11 SEM micrographs showing microstructure observed around the wall of crater in the 12 mm target, with reference to the makings in Fig. 7.

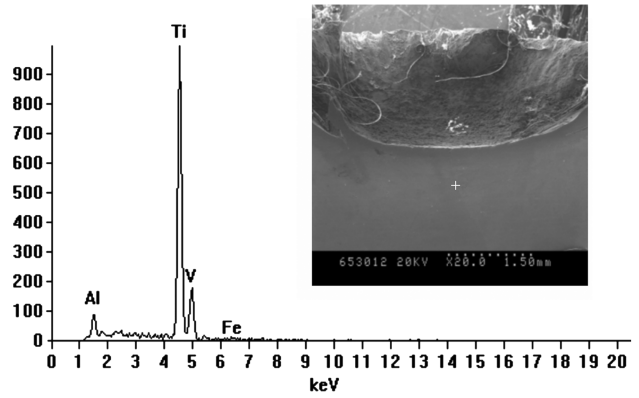

a) Referencing region on the crater wall, indicated by the cross mark

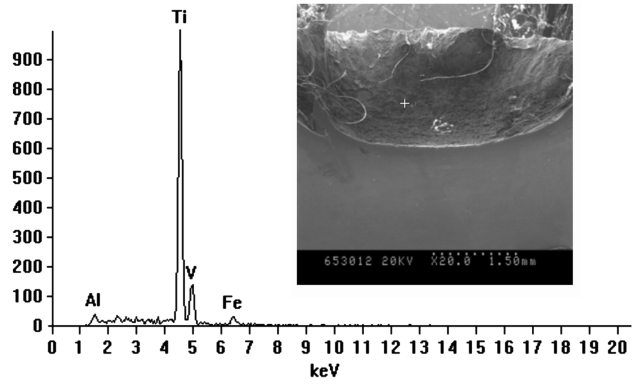

b) Bottom region inside the crater, indicated by the cross mark

Fig. 12 Spectra of energy dispersive spectrometer microanalysis of the crater formed in the 20 mm target (4 mm spherical steel projectile, impacting at a nominal velocity of 2 km/s).

4 km/s, indicating that both the crater depth and diameter increase with increasing impacting velocity. A typical hypervelocity impact crater profile, bowl-shaped crater with uniform "lips" round the edge and spalt projectile fragment in the bottom was formed and seen at a projectile velocity of about 4 km/s. As lacking of sufficient test results, a quantitative evaluation of the effect of impacting velocity cannot be currently reached on crater configuration in the Ti-6Al-4V alloy targets with different thicknesses. Further investigation is necessary and continued work is in progress.

B. Microdamage of Single Targets

Micrographic examination could provide more detailed appearance of an impacted crater and also the microdamage information of the target. Figure 7 gives the example of a low magnification scanning electron microscopy (SEM) image, viewing the cross-section of the crater in the target with thickness of 12 mm impacted at 2 km/s. The markings of "A", "B" and "C" in the photograph denote the positions of the top, middle and bottom on the crater wall, respectively. The impacting direction in which the spherical projectile travels is also shown in the photograph by an arrow. Figure 7 will be herein used as a schematic cross-section view illustrated for presentation and analysis of microdamage behavior in the single targets.

Careful examination of the craters formed in the Ti-6Al-4V alloy targets with various thicknesses at the nominal velocity of 2 km/s shows that microcracks, microvoids, localized deformation or shearing bands and adiabatic shear bands (ASBs) could be observed in the vicinity of the crater or the penetrated hole for all the checked specimens. These defects or microstructural variations are thought to be related to the microdamage in Ti-6Al-4V alloy induced by impact. Figures 8–11 display typical examples of several microdamage patterns observed either by optical microscopy or by SEM.

As is well known, the impacting process at either low-velocities or hypervelocities would lead the target undergo severe or extreme plastic deformation at a very high strain rate, producing microstructural changes in the impacted materials. It is an interesting and valuable subject to evaluate microstructure evolutions along with deformation behaviors of the target materials during the impacting process. Many efforts have been made in titanium and Ti-6Al-4V alloy to examine the localized or dynamic deformation behavior [6,7,9], recrystallization [5,6,8,9], formation of ASBs [5,6,8–10], high-strain-rate hardening [8–10,12], microstructure evolution [5,8,9] and properties variation [10,12,13] during impacting at various projectile velocities using various accelerating techniques. These studies have provided definite experimental evidences that localized deformation, formation of ASB and dynamic crystallization as well as cracking would occur in the impacted Ti-6Al-4V alloy within the damage areas. Similar phenomena were also obtained in this work by abundant microstructural observations, as represented in Figs. 8–11.

When the 4-mm-diam spherical steel impacts the single Ti-6Al-4V alloy targets at a velocity of 2 km/s, regardless of the target thickness, penetration could occur and result in cratering or perforation in a very short time through extremely sever deformation. Moreover, the sever deformation was localized at the projectile impacting circumference, usually leading to a solid-state flow of Ti-6Al-4V alloy. The matrix adjacent to the crater experiences a heavily compression and localized shear deformation, varying with the distance from the crater central, as shown in Fig. 11. For titanium alloy, shearing bands (as shown in Figs. 8 and 10) would be readily easy to form under high strain rate and high strain conditions during the crater formation. Because of the heat from the dissipation of projectile dynamic energy and extreme localized high-strain-rate deformation, the adiabatic shearing bands, as marked in Fig. 10, would reasonably form close to the cratering site. It is common for microcracks and microvoids, as, respectively, seen in Figs. 8 and 9, to nucleate and grow during the crater formation process. Several studies [6,8,9] had demonstrated by electron transmission microscopy observations that dynamic crystallization would take place as impacting the Ti-6Al-4V alloy targets at the projectile velocities of $1 \sim 2$ km/s. In the case of current study, detailed investigating in impact-induced microstructure evolutions in the single Ti-6Al-4V targets is under progress.

Table 2 Microhardness measurement of the craters with various thicknesses (4 mm spherical steel projectile, impacting at a nominal velocity of 2 km/s)[a]

Position on crater wall	Normalized hardness
2.0 mm target thickness	
Top	1.41
Middle	1.30
Bottom	1.46
5.0 mm target thickness	
Top	1.17
Middle	1.22
Bottom	1.18
7.0 mm target thickness	
Top	1.18
Middle	1.25
Bottom	1.20
10.0 mm target thickness	
Top	1.22
Middle	1.24
Bottom	1.22
Top	1.10
Middle	1.46
Bottom	1.12
20.0 mm target thickness	
Top	1.13
Middle	1.34
Bottom	1.17

[a]The bulk material microhardness of Ti-6Al-4V alloy was determined as HV312.

Another interesting microdamage phenomenon during the steel projectile impacting the Ti-6Al-4V target is the possible melting of the projectile, as shown in Fig. 12. For the crater formed in the 20 mm-thick target impacted at 2 km/s, much amount of Fe element was detected inside the bottom of the crater (as seen in Fig. 12b). The content of Fe is above 5 wt % and much higher than that in the target alloy, implying partly melting of the spherical steel projectile occurred during the impacting process. It was reported recently [17] that using of a three-stage light gas gun, the impact shock could induce vaporization of metals such as zinc, indium and aluminum with a titanium (Ti-6Al-4V) projectile traveling at 10.4 km/s. As the impacting velocity applied in this study is too low, it is reasonable to deduce the partly melting mechanism.

The microhardness distribution, around the crater cross-section in the targets with various thicknesses impacted at 2 km/s, was measured and normalized by the bulk microhardness of the target. Table 2 lists the data at the positions of top, middle and bottom of each crater, as also schematically shown in Fig. 7. The results suggest that strain hardening at high strain rates occurred in the residual crater site of Ti-6Al-4V alloy during dynamic indentation by the impacting projectile, consisting with previous studies [8–10]. The microhardness data nearby the crater wall could be used for computing simulation of the impacting process. For this sense, overall and precise measurement is necessary.

C. Damage of Multilayer Targets

The damage behaviors of the Ti-6Al-4V multilayer targets were mainly discussed and analyzed by examining the macro- and microdamage of the first and second layer plates. In practice, the investigation into damage behavior of thin metallic targets is generally for bumper sheet application [18]. Figures 13–15 show typical views of the first and second plates of the Ti-6Al-4V multilayer targets after being impacted at the nominal velocities of 1, 3 and 4 km/s, respectively. The corresponding high-magnification views of the impacted holes or perforation morphologies in the first and second plates are shown in Figs. 16–18.

It can be seen that after being impacted by a spherical steel projectile, the first layer plate of the multilayer Ti-6Al-4V alloy target was completely penetrated for all the investigated impacting-velocities, remaining remarkable perforations, as indicated by an arrow in Figs. 13a, 14a, and 15a. More detailed morphologies of the main perforations in the first layer plates can be obtained in Figs. 16a, 17a, and 18a. All the main perforations in the first layer plates impacted at velocities from 1 to 4 km/s exhibit a circular shape as well as a regular lip. Perforations look similar for the first layer plates of all targets, where the hole usually has a small lip and takes the same shape as the impacting projectile. The melting of first layer target at some point of the holes can be also found, as indicated by arrow in Figs. 16a, 17a, and 18a.

Damage in the second layer Ti-6Al-4V alloy plate seems to become much worse with the increase of impact velocity. Clean surface with only one hole for the second layer plate was seen as the projectile velocity is only 1 km/s, as shown in Fig. 13b. Increasing the velocity to 3 km/s, one main hole, with a few smaller holes around, is seen in Fig. 14b. In the case of 4 km/s projectile velocity, no remarkable main penetrated holes can be distinguished but many holes distributing widely in the second plate, as shown in Figs. 15b and 18b, indicating the formation of debris clouds after the first impact. As investigating on the impact phenomena of a thin target or shield configuration impacted by a projectile, the formation of debris clouds is usually of main concern. Formation of debris clouds is generally thought to be a result of combined effects of the impact shock wave, namely primary projectile impacting and the secondary debris impacting. Based on the preceding results and analysis, it can be concluded that the velocity might be between 3 and 4 km/s, at which the 4-mm-diam spherical steel projectile to be broken up or destroyed during impacting the Ti-6Al-4V alloy sheet targets.

It is essential to discuss and estimate the critical velocity at which the projectile would fracture or destroy when the Ti-6Al-4V alloy sheet is considered to be targets and served as thin bumpers. One investigation showed that the tungsten carbide (WC) projectile would be fractured during the impacting process at the velocity below 1.5 km/s [16]. That study was carried out on a two-stage gas

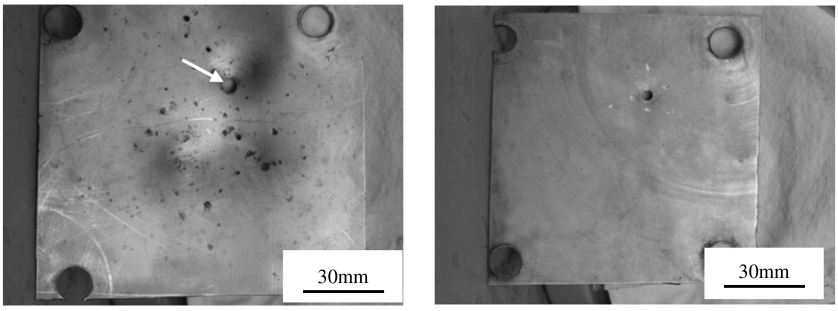

a) Front view of first layer plate **b) Front view of second layer plate**

Fig. 13 Photographs showing damage of Ti-6Al-4V multilayer target impacted at 1 km/s.

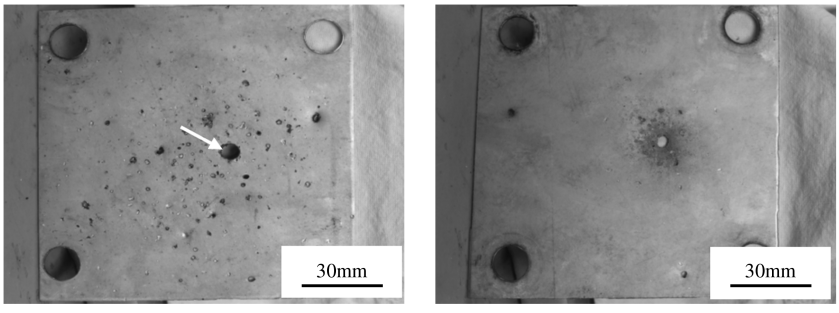

a) Front view of first layer plate **b) Front view of second layer plate**

Fig. 14 Photographs showing damage of Ti-6Al-4V multilayer target impacted at 3 km/s.

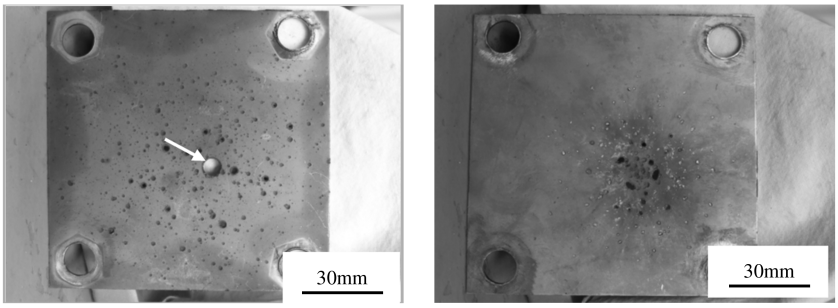

a) Front view of first layer plate b) Front view of second layer plate

Fig. 15 Photographs showing damage of Ti-6Al-4V multilayer target impacted at 4 km/s.

gun using pure titanium as a thick target and a 3 mm WC ball as a projectile. Comparing the test results from single Ti-6Al-4V alloy targets in Sec. III.A with those from multilayer targets, there is an implication that the projectile destruction depends not only on the target characteristics and impacting velocity, but also on the properties of the projectile, such as density, strength and ductility. Destroyed behavior of the projectile during hypervelocity impact is worthy of further investigation.

For the first Ti-6Al-4V plate of multilayer target impacted at 4 km/s, a typical cross-section microstructure around the penetrated

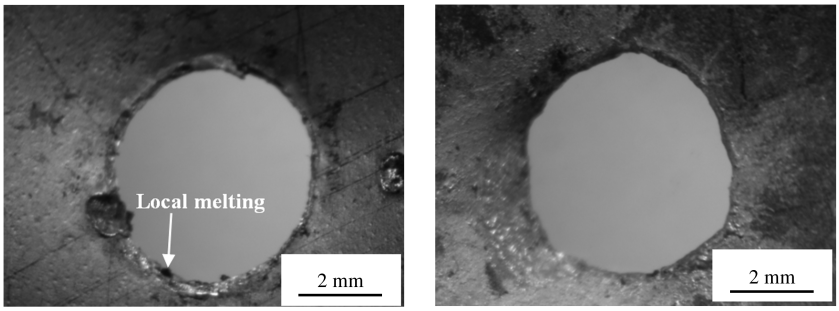

a) Hole in first layer plate b) Hole in second layer plate

Fig. 16 Enlarged views showing perforation of Ti-6Al-4V multilayer target impacted at 1 km/s.

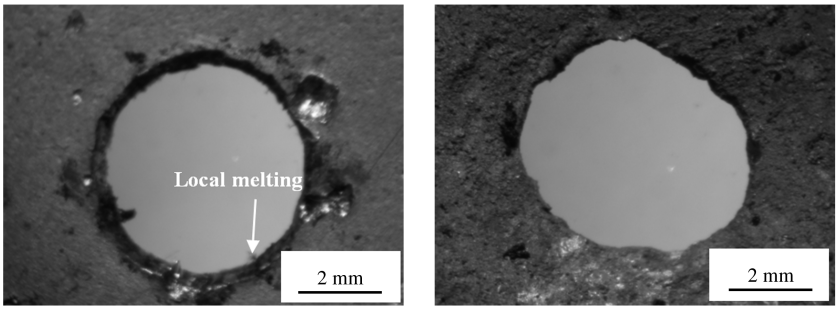

a) Hole in first layer plate b) Hole in second layer plate

Fig. 17 Enlarged views showing perforation of Ti-6Al-4V multilayer target impacted at 3 km/s.

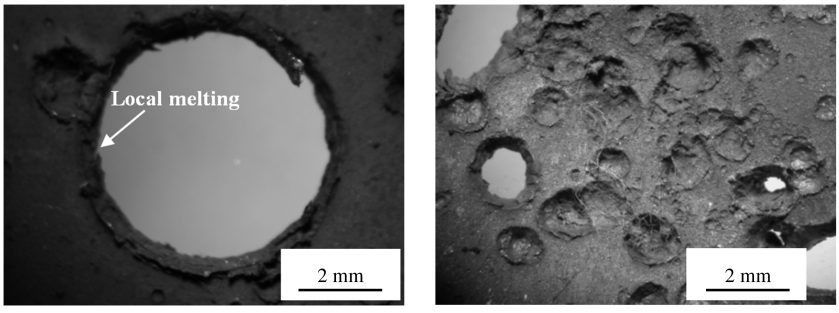

a) Hole in first layer plate b) Hole in second layer plate

Fig. 18 Enlarged views showing perforation of Ti-6Al-4V multilayer target impacted at 4 km/s.

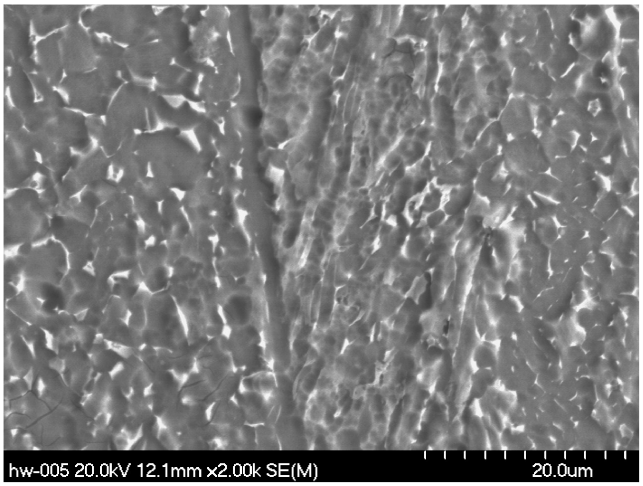

Fig. 19 SEM image showing typical microstructure features around the penetrated hole in the first Ti-6Al-4V plate of multilayer target impacted at 4 km/s.

hole along the velocity direction is shown Fig. 19.It can be seen that the microstructure is quite different from that of the impacted Ti-6Al-4V single targets, as given in Fig. 11. Such a difference arises mainly from the original microstructure difference between the annealed Ti-6Al-4V forged rods and rolled sheet. Therein, the grain size is very large for the former (several tens of micrometers) and smaller for the later (several micrometers). In addition, the difference in the impacting processes experienced in these targets could also change the damage behaviors.

IV. Conclusions

The macro- and microdamage behaviors of Ti-6Al-4V alloy have been investigated by examining the craters in targets with various thicknesses and configurations, which were impacted by 4-mm-diam spherical steel projectile at velocities varying from about 1 to 4 km/s.

For the single targets with the thickness from 2 to 20 mm, macrodamages such as the penetrated holes, impacted craters, rear surface bulging and projectile distorting or embedding in the crater were observed in the targets as increasing impact velocity from 1 to 4 km/s. The crater shape, diameter and depth were found to vary with the targets thickness and impact velocity. The threshold target thickness is about 5 mm for the annealed Ti-6Al-4V alloy to be penetrated by a 4 mm spherical projectile at 2 km/s.

The microstructural examinations demonstrated that the microvoids, microcracks, localized plastic deformations and ASBs in the region adjacent to the crater seem to be the main microdamage characteristics in the single targets, depending on target thickness and impact velocity. Microhardness in the region close to the crater is much higher than that far from the crater, implying the occurrence of drastically localized plastic deformation inside and around the crater during impact process.

As impacted by the spherical steel projectile at velocities from 1 to 4 km/s, the first layer plate of the multilayer Ti-6Al-4V alloy targets was damaged in a mode of forming a penetrated hole. A trace of partly melting of target matrix alloy was detected along the perimeter of the impacted hole, and small cracks could be seen inside the wall of the penetrated hole. The damage in the second layer plate was found to become more severe with increasing impact velocity, due to the combined effects caused by impact shock waves, original projectile impact and the secondary debris impact.

Large area damage induced by debris clouds impact in the second layer plate was observed for the multilayer targets impacted at 4 km/s, while not remarkable at 3 km/s. Reminding of the crater features formed in the single targets, it is indicated that as the Ti-6Al-4V alloy is the target, the critical velocity to break up the 4-mm-diam spherical steel projectile should be between 3 and 4 km/s.

Acknowledgment

The authors would like to acknowledge support by the National Nature Science Foundation of China under the contract of 50431020.

References

[1] Leyens, C., and Perters, M., *Titanium and Titanium Alloys: Fundamentals and Applications*, 1st ed., WILEY-VCH Publishers, Germany, 2002, Chap. 13.

[2] Ashraf Imam, M., "The 11th World Conference on Titanium (Ti-2007)," *JOM*, Vol. 60, No. 5, 2008, p. 40. doi:10.1007/s11837-008-0058-3

[3] Lai, S. T., Murad, E., and McNei, W. J., "Hazards of Hypervelocity Impacts on Spacecraft," *Journal of Spacecraft and Rockets*, Vol. 39, No. 1, 2002, pp. 106–114. doi:10.2514/2.3788

[4] Jantou, V., McPhail, D. S., Chater, R. J., and Kearsley, A., "Analysis of Simulated Hypervelocity Impacts on a Titanium Fuel Tank from the Salyut 7 Space Station," *Applied Surface Science*, Vol. 252, No. 19, 2006, pp. 7120–7123. doi:10.1016/j.apsusc.2006.02.212

[5] Li, H. T., Zhang, Y. M., and Yang, D. Z., "Microdamage of Ti-6Al-4V Alloy Under Hypervelocity Projectile Impact," *Materials Science and Engineering A*, Vol. 292, No. 1, 2000, pp. 130–132. doi:10.1016/S0921-5093(00)01019-4

[6] Li, G. A., Zhen, L., Lin, C., Gao, R. S., Tan, X., and Xu, C. Y., "Deformation Localization and Recrystallization in TC4 Alloy Under Impact Condition," *Materials Science and Engineering A*, Vol. 395, Nos. 1–2, 2005, pp. 98–101. doi:10.1016/j.msea.2004.12.020

[7] Lee, D. G., Kim, Y. G., Nam, D. H., Hur, S. M., and Lee, S., "Dynamic Deformation Behavior and Ballistic Performance of Ti-6Al-4V Alloy Containing Fine α_2 (Ti_3Al) Precipitates," *Materials Science and Engineering A*, Vol. 391, No. 1, 2005, pp. 221–234. doi:10.1016/j.msea.2004.08.076

[8] Martinez, F., Murr, L. E., Ramirez, A., Lopez, M. I., and Gaytan, S. M., " Dynamic Deformation and Adiabatic Shear Microstructures Associated with Ballistic Plug Formation and Fracture in Ti-6Al-4V Targets," *Materials Science and Engineering A*, Vols. 454–455, No. 25, April 2007, pp. 581–589. doi:10.1016/j.msea.2006.11.097

[9] Murr, L. E., Ramirez, A. C., Gaytan, S. M., Lopez, M. I., Martinez, E. Y., Hernandez, D. H., and Martinez, E., "Microstructure Evolution Associated with Adiabatic Shear Bands and Shear Band Failure in Ballistic Plug Formation in Ti-6Al-4V Targets," *Materials Science and Engineering A*, Vol. 516, Nos. 1–2, 2009, pp. 205–216. doi:10.1016/j.msea.2009.03.051

[10] Me-Bar, Y., and Rosenberg, Z., "On the Correlation Between the Ballistic Behavior and Dynamic Properties of Titanium-Alloy Plates, " *International Journal of Impact Engineering*, Vol. 19, No. 4, 1997, pp. 311–318. doi:10.1016/S0734-743X(96)00046-2

[11] Atroshenkoa, S. A., Naumovaa, N. S., and Novikovb, S. A., "Influence of High-Velocity Impact on Metals," *International Journal of Impact Engineering*, Vol. 33, Nos. 1–12, 2006, pp. 62–67. doi:10.1016/j.ijimpeng.2006.09.020

[12] Meyer, H. W., and Kleponis, D., "Modeling the High Strain Rate Behavior of Titanium Undergoing Ballistic Impact and Penetration," *International Journal of Impact Engineering*, Vol. 26, Nos. 1–10, 2001, pp. 509–521. doi:10.1016/S0734-743X(01)00107-5

[13] Walters, W., Gooch, W., and Burkins, M., "The Penetration Resistance of a Titanium Alloy Against Jets from Tantalum Shaped Charge Liners," *International Journal of Impact Engineering*, Vol. 26, Nos. 1–10, 2001, pp. 823–830. doi:10.1016/S0734-743X(01)00135-X

[14] Baker, J. R., "Hypervelocity Crater Penetration Depth and Diameter: A Linear Function of Impact Velocity?," *International Journal of Impact Engineering*, Vol. 17, Nos. 1–3, 1995, pp. 25–35. doi:10.1016/0734-743X(95)99832-C

[15] Valerio-Flores, D. L., Murr, L. E., Hernandez, V. S., and Quinones, S. A., "Observations and Simulations of the Low Velocity-to-Hypervelocity Impact Crater Transition for a Range of Penetrator Densities into Thick Aluminum Targets," *Journal of Materials Science*, Vol. 39, No. 20, 2004, pp. 6271–6289. doi:10.1023/B:JMSC.0000043597.72588.d1

[16] Oka, Y. I., Nagahashi, K., Ishii, Y., Kobayashi, Y., and Tsumura, T., " Damage Behaviour of Metallic Materials Caused by Subsonic to

Hypervelocity Particle Impact," *Wear*, Vol. 258, Nos. 1–4, 2005, pp. 100–106. doi:10.1016/j.wear.2004.04.013

[17] Chhabildas, L. C., Reinhart, W. D., Thornhill, T. F., and Brown, J. L., "Shock-Induced Vaporization in Metals," *International Journal of Impact Engineering*, Vol. 33, Nos. 1–12, 2006, pp. 158–168. doi:10.1016/j.ijimpeng.2006.09.014

[18] Higashide, M., Tanaka, M., Akahoshi, Y., Harada, S., and Tohyama, F., "Hypervelocity Impact Tests Against Metallic Meshes," *International Journal of Impact Engineering*, Vol. 33, Nos. 1–12, 2006, pp. 335–342. doi:10.1016/j.ijimpeng.2006.09.071

D. Edwards
Associate Editor